Single-Mode High-Speed 1550 nm Wafer Fused VCSELs for Narrow WDM Systems

Andrey Babichev, Sergey Blokhin, Andrey Gladyshev, Leonid Karachinsky, Innokenty Novikov, Alexey Blokhin, Mikhail Bobrov, Nikolay Maleev, Vladislav Andryushkin, Evgenii Kolodeznyi, Dmitrii Denisov, Natalia Kryzhanovskaya, Kirill Voropaev, Victor Ustinov, Anton Egorov, Hui Li, Si-Cong Tian, *Member, IEEE*, Saiyi Han, Georgiy Sapunov, and Dieter Bimberg, *Life Fellow, IEEE*

***Abstract*— High power single-mode wafer fused 1550 nm VCSELs with an active region based on InGaAs quantum wells are fabricated. An InP-based optical cavity and two AlGaAs/GaAs distributed Bragg reflector heterostructures were grown by molecular-beam epitaõy. The current and optical confinements are provided by a lateral-structured buried tunnel junction with ∼ 6 μm diameter and etching depth of ∼ 20 nm. The VCSELs demonstrate ∼ 3.4 mW single-mode continuous-wave output optical power and a threshold current about 2 mA at 20°C. The output optical power exceeds 1 mW at 70°C. A −3dB modulation bandwidth > 13 GHz is obtained at 20°C. Non-return-to-zero data transmission under back-to-back condition of ∼ 37 Gbps is shown.**

***Index Terms*— Vertical-cavity surface-emitting lasers (VCSELs), wafer fusion, optical modulation, InP, optical interconnects.**

Manuscript received 21 December 2022; revised 12 January 2023; accepted 27 January 2023. Date of publication 1 February 2023; date of current version 9 February 2023. This work was supported in part by the CAS through the CAS Youth Innovation Promotion Association through the for the Large Signal Modulation Measurements under Grant 2018249, in part by the ITMO University through the Static Characteristics Measurements under Project 2019-1442, and in part by the Priority 2030 Program for the Small Signal Modulation Experiments. The work of Sergey Blokhin and Leonid Karachinsky was supported by the Chinese Academy of Sciences (CAS) President's International Fellowship Initiative (PIFI) Program for the Analysis of the Static Characteristics and Small Signal Modulation Characteristics. The work of Natalia Kryzhanovskaya was supported by the Basic Research Program of the National Research University Higher School of Economics for Support of Optical Spectra Measurements. *(Corresponding authors: Andrey Babichev; Si-Cong Tian.)*

Andrey Babichev, Andrey Gladyshev, Leonid Karachinsky, Innokenty Novikov, Vladislav Andryushkin, and Evgenii Kolodeznyi are with ITMO University, 197101 Saint Petersburg, Russia (e-mail: a.babichev@itmo.ru).

Sergey Blokhin, Alexey Blokhin, Mikhail Bobrov, and Nikolay Maleev are with the Ioffe Institute, 194021 Saint Petersburg, Russia.

Dmitrii Denisov and Anton Egorov are with Alferov University, 194021 Saint Petersburg, Russia.

Natalia Kryzhanovskaya is with the Higher School of Economics, National Research University, 190008 Saint Petersburg, Russia.

Kirill Voropaev is with Yaroslav-the-Wise Novgorod State University, 173003 Veliky Novgorod, Russia.

Victor Ustinov is with the Submicron Heterostructures for Microelectronics Research and Engineering Center, Russian Academy of Sciences (RAS), 194021 Saint Petersburg, Russia.

Hui Li is with the College of Mathematical and Physical Sciences, Qingdao University of Science and Technology, Qingdao 266100, China.

Si-Cong Tian, Saiyi Han, Georgiy Sapunov, and Dieter Bimberg are with the Bimberg Chinese-German Center for Green Photonics, Changchun Institute of Optics, Fine Mechanics and Physics (CIOMP), Chinese Academy of Sciences (CAS), Changchun 130033, China, and also with the Center of Nanophotonics, Institute of Solid State Physics, Technische Universität Berlin, 10623 Berlin, Germany (e-mail: tiansicong@ciomp.ac.cn).

Color versions of one or more figures in this letter are available at https://doi.org/10.1109/LPT.2023.3241001.

Digital Object Identifier 10.1109/LPT.2023.3241001

I. Introduction

THE infrastructure of more recent data centers is emerging to a coexistence between multimode fibers and single-mode fibers (SMF) enabling WDM (Wavelength-Division Multiplexing) solutions. Thus, both larger capacity and longer reach is achieved as the data centers grow in both size and traffic [1], [2]. The spectral efficiency of data center networks can be further increased by using SDM (Spatial Division Multiplexing) technique based on multicore fibers (MCF) or few-mode fibers (FMF) [3], [4], [5]. Moreover, LW SM VCSELs reduce the negative effect of modal and chromatic dispersion in an optical link. As a result, C-band VCSELs are promising for next generation giga data centers, where optical links based on SM fibers with longer transmission distances are important, in particular for wavelength multiplexing [6]. Additionally, SDM transmission through MCFs using long-wavelength (LW) VCSELs are enabling large-scale data center networks [7]. Therefore, 1550 nm SM VCSELs show a great potential not only for next-generation short-reach optical interconnects,but also for SDM transceivers. A 50+ Gbps per channel capacity up to 116 km distance based on direct modulated 1550 nm VSCEL with discrete multitoned format has been demonstrated [8]. Moreover, a 200-Gbps transmission over 100-meter multi-mode fiber with direct detection and 28-km few-mode fiber using a 1550 nm 2-D VCSEL matrix with coherent detection were presented as well [9]. The development of the monolithic (grown in a single epitaxial process) LW VCSELs is challenging due to critical limitations inherent to InAlGaAsP/InP [10] and InAlGaAs/GaAs material systems.

There are two major technologies for the fabrication of high-speed 1550 nm VCSELs, actively using a buried tunnel junction (BTJ) concept (both schematically represented in Ref. 11). The first one involves a hybrid integration of an InP-based optical cavity with dielectric distributed Bragg reflectors (DBR) [12], [13], [14], [15], [16]. One of the unique features of the VCSELs developed by the Vertilas/TUM team is to use thick (about 50 μm) galvanic gold as a substrate. The second one involves direct wafer fusion (WF) of an InP-based optical cavity with two GaAs-based DBRs [17], [18]. The EPFL team fabricated full wafers of WF VCSELs

using double WF technology, which demonstrates that WF VCSEL technology is compatible with standard industrial manufacturing processes [17], [19], [20] being attractive for high volume production [21]. Moreover, the second approach allows realizing the reliable LW VCSELs, satisfying GR-468-CORE Telcordia qualification test [22].

In the frame of the first approach, the highest small-signal modulation bandwidth in excess of 20 GHz at 25°C and error-free uncooled performance up to 50 Gbps in back-to-back configuration without equalization or forward error correction [15] achieved up-to-date for a short-cavity VCSEL design [13] and 14. For the devices operating at the modulation bandwidth of about 22 GHz the SM output optical power is about 1.6–2.4 mW [7], [16], [23], [24]. This superior dynamic performance is due to the combination of ultra-short semiconductor cavity (∼1.5-μm) and two high-index contrast DBRs (dielectric, AlF_3/ZnS top and hybrid, AlF_3/ZnS-Au based, back mirrors) [7] with a small penetration depth (300 nm [15]), which allows one to minimize the mode volume and increase the *D*-factor. Moreover, double-mesa devices with flip-chip process to minimize the mesa capacitance (aimed at increase the parasitic frequency) and thermal issue (aimed at improve heat spreading) were used [16]. In the frame of the second approach involving WF, due to the effective combination of the advantages of both InAlGaAs/InP and AlGaAs/GaAs material systems it was managed to demonstrate high SM output optical power of more than 6 mW at 20°C [17], [18], [25]. The higher SM output optical power of WF VCSELs compared to short-cavity VCSELs is related with better thermal conductivity of GaAs-based DBRs in relation with dielectric DBRs. In fact, the thermal resistance is about 5 times higher for short-cavity VCSELs [15] in relation to the WF VCSELs [17] with the same BTJ diameter. The modest high-speed performance of 1550 nm range WF VCSELs [18], [25], [26] is noticeably inferior to short-cavity VCSELs. It is related with long cavity (∼3λ) as well as device topology in relation with short-cavity VCSELs.

In this Letter, we report on continuous-wave (CW) and dynamic characteristics of 1550 nm SM VCSELs, fabricated by direct bonding of MBE-grown wafers. Usage of optimized both structure design with active region based on thin strained InGaAs/InAlGaAs quantum wells (QWs) as well as VCSEL device topology allowed to enhance the -3dB modulation bandwidth up to 13 GHz and demonstrate 37 Gbps non-return-to-zero (NRZ) direct modulation at room temperature, which is the largest date rate for 1550 nm WF VCSELs until now to the best of our knowledge.

II. VCSEL Structure and Fabrication

The VCSEL design includes a vertical cavity with undoped semiconductor DBRs, BTJ for transverse current/optical confinement, and n-type intracavity contacts [18]. The VCSEL structure consists of AlGaAs/GaAs DBR wafers fused to both sides of the InAlGaAs/InP cavity, using our previously described technology [25], [26], [27], [28]. The optical cavity and DBR structures were grown by MBE on a Riber 49 production system at Connector Optics LLC. The top and bottom DBRs were grown on GaAs substrates and consist of 22.5 and 35.5 pairs of $Al_{0.9}Ga_{0.1}As$/GaAs layers, respectively.

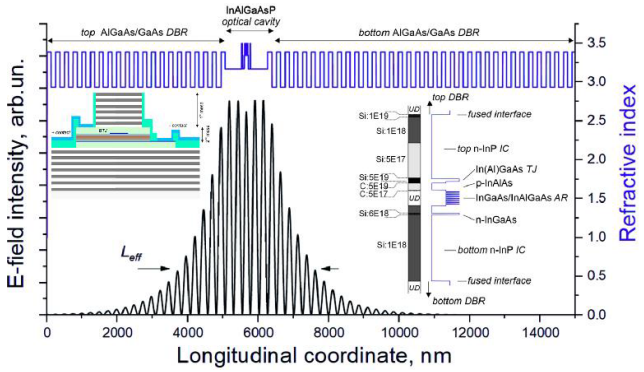

Fig. 1. Vertical distribution of electromagnetic field intensity along the refractive index and doping profiles. The inset shows schematic cross-section of device.

The InAlGaAs/InP cavity was grown on an InP substrate and consist of the bottom n-InP intra cavity (IC) layer with a highly doped n-InGaAs contact layer, an active region, a p-InAlAs emitter, a composite In(Al)GaAs TJ, selectively overgrown by InP layer to form the BTJ mesa, and a top n-InP IC layer with a highly doped contact layer. The length of the optical cavity is 3λ (cf. Figure 1).

There are some principal changes in design of VCSEL structure in relation with our previous MBE-grown 1550 nm WF VCSELs [25]. First, the number of thin $In_{0.74}Ga_{0.26}As$

QWs was increased from 7 to 10 in order to increase total modal gain. Second, it was decreased the $In_{0.53}Al_{0.16}Ga_{0.31}As$ barrier thickness from 12 nm to 7 nm, as a result the total mechanical strain in the InGaAs QW-based active region was increased up to 0.36% in relation with the previous value (0.27%). In opposite to metalorganic vapour-phase epitaxy grown (MOVPE-grown) WF VCSELs [18] no strain compensation in barriers was used. Third, the both highly-doped contact layers were changed: bottom n-InGaAs layer was used instead of n-InGaAsP, and top n-InP layer was used instead of n-InGaAsP. This was done to improve the serial resistance and precision opening of contact layers during wet etching. Fourth, the composite In(Al)GaAs BTJ: the $n^{++}/p^{++}/p^{++}$ 37 nm-thick $In_{0.53}Ga_{0.47}As/In_{0.53}Ga_{0.47}As/In_{0.53}Al_{0.16}Ga_{0.31}As$ TJ was used instead of n^{++}/p^{++} 35 nm-thick $In_{0.53}Al_{0.20}Ga_{0.27}As$ TJ [18]. In addition, the doping level of n-InP overgrowth layer was reduced as well.

The VCSEL processing steps include dry etching of the top DBR mesa (1st mesa) using inductively coupled plasma, two-step selective wet etching of the InAlGaAsP/InP optical cavity (2nd mesa), plasma enhanced chemical vapor deposition of Si_3N_4 (see Figure 1). The Ti/Pt/Au metallization for both contacts is formed by a lift-off process. Ground-source-ground contact pads were placed on the top surface level. To improve the dynamic device performance, we used small-type device topology. The mesa sizes were significantly smaller in relation with previous MBE-grown 1550 nm WF VCSEL design [25] in order to provide less parasitic capacitance of the fabricated VCSELs because capacitance C_p increases with the mesa size. The diameter of the 1st mesa was fixed to be about 12 μm, while the sizes of the 2nd mesa were reduced to ∼22 × 17 μm (cf. Figure 1, inset). As result, both the structure design as well as the mesa design were modified aimed to improve

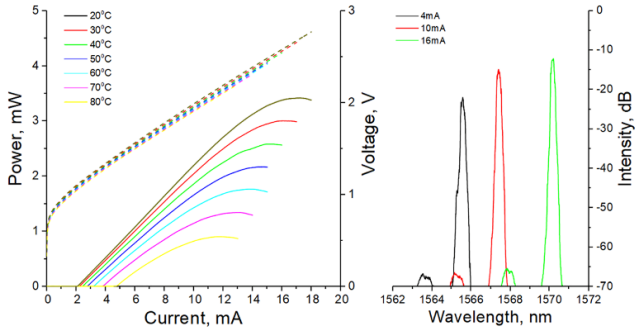

Fig. 2. CW LIV characteristics measured at 20– 90°C and the lasing spectra at 20°C and at various drive currents.

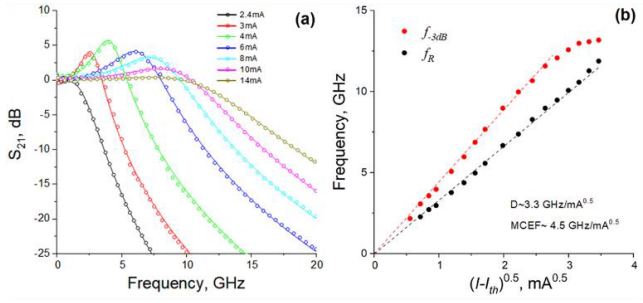

Fig. 3. (a) Measured (points) small signal modulation response S_{21} and the corresponding curve-fits (solid lines) for different drive currents; (b) relaxation resonance frequency f_R and −3dB modulation bandwidth f_{-3dB} as function of the squared root of the drive current above threshold. The temperature of measurements was 20°C.

the dynamic device performance in relation with previously MBE-grown 1550 nm WF VCSELs [25].

III. VCSEL Characterization

A. Static Characteristics

The CW light-current-voltage (LIV) characteristics measured at various heatsink temperatures are shown in Figure 2. At 20°C the lasers demonstrate CW operation with a threshold current of less than 2.1 mA and a differential efficiency of more than 0.27 W/A (equivalent to ∼21%). The threshold voltage is 1.1 V. The maximum wall plug efficiency (WPE) is ∼ 11%. The maximum output optical power of about 3.4 mW was achieved at 17 mA. The lasing spectra measured at 20°Ñ demonstrate single-mode lasing with a side mode suppression ratio (SMSR) of more than 45 dB (cf. Figure 2, right panel). Note that high-speed 1550 nm hybrid short-cavity VCSELs based on thick InAlGaAs QWs and n^+-InGaAs/p^+-In(Al)GaAs BTJ demonstrate SM lasing only for BTJ apertures less than 5 μm, while the maximum SM output optical power (SMSR ≥ 40 dB) does not exceed 2.4 mW, which is associated with a strong waveguide effect in such a laser structure [16]. At 70°C we observed a decrease in the maximum output optical power to ∼ 1 mW accompanied by a threshold current increase to 3.9 mA. The maximum WPE value at 70°C is 6%. The estimated value of the maximum lasing temperature is about 95°C.

B. Small Signal Modulation

Electrical reflection (S_{11} parameter) and small-signal modulation response (S_{21} parameter) were measured using a Rodhe & Schwarz ZVA 40 network analyzer and a 25 GHz New Focus 1434 photodetector. To extract the key intrinsic parameters of the VCSEL, we used a three-pole transfer function describing the laser response to sinusoidal modulation of the drive current at a certain frequency f: $H(f) \propto f_R^2/(f_R^2 - f^2 + j\gamma(f/2\pi))(1 + j(f/f_p))$, where f_R is the relaxation resonance frequency, γ is the intrinsic damping factor (damping), f_p is the parasitic cutoff frequency of the low-frequency filter formed by the capacitors and resistances of the laser. The results of small-signal frequency analysis and the intrinsic modulation parameters extracted from the measured $S_{21}(f)$ at 20 °C are shown in Figure 3. The extracted −3dB modulation bandwidth f_{-3dB} (at which frequency response drops by -3 dB) reaches 12 GHz at a drive current of more than 10 mA with a modulation current efficiency (expressed by MCEF $= f_{-3dB}/(I - I_{th})^{0.5}$) of 4.5 GHz/(mA)$^{0.5}$ (see Figure 3(b)). The relaxation resonance frequency f_R does not exceed the -3dB modulation bandwidth in the whole current range. The rate of increase of the f_R with the square root of the drive current above lasing threshold, the so-called D-factor, reflecting the level of differential gain and mode volume (expressed by $D = f_R/(I - I_{th})^{0.5}$), reaches 3.3 GHz/(mA)$^{0.5}$.

At moderate photon densities the intrinsic damping factor γ on the square of the relaxation resonance frequency f_R^2 dependence can be well described by a linear function ($\gamma = Kf_R^2 + \gamma_0$). The K-factor reaches 0.45 ns, which is larger than that for 1550 nm VCSELs based on thick InAlGaAs QWs and InAlGaAs TJ [18] and 1550 nm WF VCSELs based on InGaAs QWs and InAlGaAs TJ [27] showing similar differential efficiencies.

In case of dominance of damping, the maximum theoretically achievable modulation bandwidth is estimated to be 20 GHz, while in the case of dominance of thermal effects, the maximum theoretically achievable modulation bandwidth does not exceed 18 GHz. Modeling the frequency dependence $S_{11}(f)$, showed a strong decrease in the parasitic capacitance of the reverse-biased p^+n-junction region due to a significant reduction in the 2nd mesa size, which made it possible to increase the parasitic cut-off frequency up to 13–14 GHz. As clearly shown in Figure 3(a), the frequency response becomes overdamped at high photon density (more than 10 mA).

Note that these values present a record for 1550 nm VCSELs fabricated by the WF technology, regardless of the active region type or TJ use [18], [25], [26]. It should be noted that these results are inferior to the results obtained for a 1550 nm hybrid short-cavity VCSELs [16], where the device design allows not only to minimize the parasitic capacitance, but also to significantly reduce the mode volume.

C. Large Signal Modulation

To study large signal modulation performance of 1550 nm WF VCSELs the signal was generated by a SHF 12105A bit pattern generator, amplified by a SHF 827B amplifier followed by a tunable 3 dB attenuator. A pseudorandom binary sequence with a word length of 27^{-1} was chosen. The emission of the VCSEL was coupled to the cleaved end of a 3 meter SMF. An isolator was used to suppress optical reflections. A 42 GHz Thorlabs RXM42AF optical probe was used to convert the oscilloscope. In Figure 4, we present large signal modulation measurement results at 20 °C. Clear open eye diagrams (left-hand side of Figure 4) are obtained. The bit-error ratio (BER) characteristics for crosstalk (bath tub curves), which are shown on the right-hand side of Figure 4 can be used to extract the jitter. By applying 16 mA bias current and 300 mV modulation voltage, a record NRZ data rate for WF 1550 nm

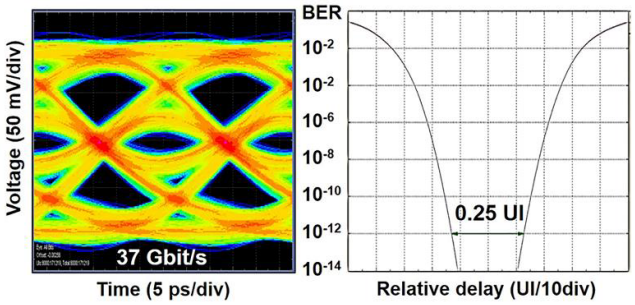

Fig. 4. Eye diagram (left) and bit error ratio (right) bath tub curve for a data rate of 37 Gbps across a 3 m SMF. The temperature of measurements was 20°C.

VCSELs of 37 Gbps under back-to-back (BTB) condition was observed (left-hand side in Figure 4). We observe 0.25 UI (6.75 ps) of eye opening and 75% total jitter (20.27 ps) at BER=10^{-12} (right-hand side in Figure 4). Previously data rates up to 25 Gbps has been presented for MBE-grown 1550 nm WF VCSELs [25]. Moreover, for MOVPE-grown 1550 nm WF VCSELs the modulation performance is modest (approximately 10 Gbps [18]).

IV. Conclusion

Both the structure design as well as the mesa design were modified aimed to improve the dynamic device performance of MBE-grown 1550 nm WF VCSELs. The composite In(Al)GaAs BTJ has been optimized both in terms of enabling MBE-overgrowth of the surface relief formed in TJ and in terms of achieving a compromise between the small mode volume and the high SM output optical power. Doping of the overgrown n-InP layer was selected to achieve a compromise between low electrical resistance and high parasitic cut-off frequency. Decrease of parasitic capacitance of the reverse-biased p^+n-junction region outside the BTJ region allowed to raise the parasitic cut-off frequency up to 13–14 GHz, therefore, the key mechanism limiting the high-speed performance of such devices is damping of the relaxation oscillation. As a result, VCSELs with optimized both the structure design as well as device topology have shown more than 13 GHz modulation bandwidth and a 37 Gbps NRZ data transmission under BTB condition. The large output optical power and dynamic characteristics of studied 1550 nm InGaAs QW-based WF VCSELs indicate their potential for large distance transmission (e.g. 1 km), where a high bit rate keeping SM behavior is necessary in order to operate narrow WDM systems (e.g. 5 nm distance).

Further increase of modulation performance can be related with decrease the parasitic capacitance (by optimization of the top n-InP IC layer doping profile [28]) as well as photon lifetime adjustment (by changing the top DBR reflectivity) [18], [25].

References

[1] I. Kanakis et al., "High-speed VCSEL-based transceiver for 200 GbE short-reach intra-datacenter optical interconnects," *Appl. Sci.*, vol. 9, no. 12, p. 2488, Jun. 2019.

[2] *Datacenters to Get a High Fiber Bandwidth Diet*. Accessed: Jan. 28, 2023. [Online]. Available: https://www.nextplatform.com/2016/03/18/datacenters-get-high-fiber-bandwidth-diet/

[3] L. Zhang, J. Chen, E. Agrell, R. Lin, and L. Wosinska, "Enabling technologies for optical data center networks: Spatial division multiplexing," *J. Lightw. Technol.*, vol. 38, no. 1, pp. 18–30, Jan. 15, 2020.

[4] A. Liu, P. Wolf, J. A. Lott, and D. Bimberg, "Vertical-cavity surface-emitting lasers for data communication and sensing," *Photon. Res.*, vol. 7, no. 2, p. 121, Jan. 2019.

[5] J. C. Charlier and S. Krüger, "Long-wavelength VCSELs ready to benefit 40/100-GbE modules," *Lightwave*, vol. 28, no. 6, pp. 2–7, Jan. 2012. Accessed: Jan. 28, 2023. [Online]. Available: https://www.lightwaveonline.com/optical-tech/article/16649511/longwavelength-vcsels-ready-to-benefit-40100gbe-module

[6] D. M. Kuchta et al., "Error-free 56 Gb/s NRZ modulation of a 1530-nm VCSEL link," *J. Lightw. Technol.*, vol. 34, no. 14, pp. 3275–3282, Jul. 15, 2016.

[7] L. Zhang et al., "Nonlinearity tolerant high-speed DMT transmission with 1.5-μm single-mode VCSEL and multi-core fibers for optical interconnects," *J. Lightw. Technol.*, vol. 37, no. 2, pp. 380–388, Jan. 15, 2019.

[8] M. Rapisarda et al., "Impact of SOA-based add-drop switch nodes on high-capacity multicarrier transmission for metro-access networks," *J. Lightw. Technol.*, vol. 40, no. 14, pp. 4492–4501, Apr. 15, 2022.

[9] C. Li et al., "Co-packaged optics with multimode fiber interface employing 2-D VCSEL matrix," *J. Lightw. Technol.*, vol. 40, no. 10, pp. 3325–3330, Mar. 15, 2022.

[10] M.-R. Park, O.-K. Kwon, W.-S. Han, K.-H. Lee, S.-J. Park, and B.-S. Yoo, "All-epitaxial InAlGaAs-InP VCSELs in the 1.3–1.6-μm wavelength range for CWDM band applications," *IEEE Photon. Technol. Lett.*, vol. 18, no. 16, pp. 1717–1719, Aug. 15, 2006.

[11] E. Kapon and A. Sirbu, "Power-efficient answer," *Nature Photon.*, vol. 3, no. 1, pp. 27–29, Jan. 2009.

[12] W. Hofmann et al., "22-Gb/s long wavelength VCSELs," *Opt. Exp.*, vol. 17, no. 20, Sep. 2009, Art. no. 17547.

[13] W. Hofmann, "High-speed buried tunnel junction vertical-cavity surface-emitting lasers," *IEEE Photon. J.*, vol. 2, no. 5, pp. 802–815, Oct. 2010.

[14] M. Müller et al., "1550-nm high-speed short-cavity VCSELs," *IEEE J. Sel. Topics Quantum Electron.*, vol. 17, no. 5, pp. 1158–1166, Oct. 2011.

[15] S. Spiga et al., "Single-mode high-speed 1.5-μm VCSELs," *J. Lightw. Technol.*, vol. 35, no. 4, pp. 727–733, Aug. 15, 2017.

[16] S. Spiga, D. Schoke, A. Andrejew, G. Boehm, and M.-C. Amann, "Effect of cavity length, strain, and mesa capacitance on 1.5-μm VCSELs performance," *J. Lightw. Technol.*, vol. 35, no. 15, pp. 3130–3141, Aug. 1, 2017.

[17] A. Caliman, A. Mereuta, G. Suruceanu, V. Iakovlev, A. Sirbu, and E. Kapon, "8 mW fundamental mode output of wafer-fused VCSELs emitting in the 1550-nm band," *Opt. Exp.*, vol. 19, no. 18, p. 16996, Aug. 2011.

[18] D. Ellafi et al., "Control of cavity lifetime of 15 μm wafer-fused VCSELs by digital mirror trimming," *Opt. Exp.*, vol. 22, no. 26, Dec. 2014, Art. no. 32180.

[19] D. Ellafi et al., "Effect of cavity lifetime variation on the static and dynamic properties of 1.3-μm wafer-fused VCSELs," *IEEE J. Sel. Topics Quantum Electron.*, vol. 21, no. 6, pp. 414–422, Dec. 2015.

[20] A. Mereuta et al., "Increasing single mode power of 13-μm VCSELs by output coupling optimization," *Opt. Exp.*, vol. 23, no. 9, Apr. 2015, Art. no. 10900.

[21] V. Iakovlev et al., "Progress and challenges in industrial fabrication of wafer-fused VCSELs emitting in the 1310 nm band for high speed wavelength division multiplexing applications," *Proc. SPIE*, vol. 8639, Mar. 2013, Art. no. 863904.

[22] A. Sirbu et al., "Reliability of 1310 nm wafer fused VCSELs," *IEEE Photon. Technol. Lett.*, vol. 25, no. 16, pp. 1555–1558, Aug. 15, 2013.

[23] J. Van Kerrebrouck et al., "High-speed PAM_4-based optical SDM interconnects with directly modulated long-wavelength VCSEL," *J. Lightw. Technol.*, vol. 37, no. 2, pp. 356–362, Jan. 15, 2019.

[24] S. Spiga, D. Schoke, A. Andrejew, M. Müller, G. Boehm, and M.-C. Amann, "Single-mode 1.5-μm VCSELs with 22-GHz small-signal bandwidth," in *Proc. Opt. Fiber Commun. Conf. Exhib. (OFC)*, Mar. 2016, pp. 1–3.

[25] A. V. Babichev et al., "6-mW single-mode high-speed 1550-nm wafer-fused VCSELs for DWDM application," *IEEE J. Quantum Electron.*, vol. 53, no. 6, pp. 1–8, Dec. 2017.

[26] S. A. Blokhin et al., "Influence of output optical losses on the dynamic characteristics of 1.55-μm wafer-fused vertical-cavity surface-emitting lasers," *Semiconductors*, vol. 53, no. 8, pp. 1104–1109, Aug. 2019.

[27] S. Blokhin et al., "Wafer-fused 1300 nm VCSELs with an active region based on superlattice," *Electron. Lett.*, vol. 57, no. 18, pp. 697–698, Jun. 2021.

[28] S. A. Blokhin et al., "High power single mode 1300-nm superlattice based VCSEL: Impact of the buried tunnel junction diameter on performance," *IEEE J. Quantum Electron.*, vol. 58, no. 2, pp. 1–15, Apr. 2022.